Passive House Performance in Cold Climates: a Review of the Envelope Performance and Energy Consumption of a Certified Research and Testing Facility in Canada

A. Conroy[a*], G. Wimmers[b]

[a] PhD candidate, University of Northern British Columbia, Canada, conroy@unbc.ca
[b] Associate Professor, University of Northern British Columbia, Canada, guido.wimmers@unbc.ca

Abstract:
The University of Northern British Columbia's Wood Innovation Research Lab (WIRL) is the first industrial facility tested and certified to the International Passive House standard in Canada. Constructed using a glulam post and beam system and unique high-performance standing truss wall assembly, the building serves as a research and testing facility for University faculty and students. Temperature and humidity sensors were installed in the north and south wall façade during construction to measure the building's hygrothermal performance. In addition, energy consumption meters were installed to measure the annual energy and heating demand of the building. Both the hygrothermal performance and energy use data are of interest due to the unique envelope design, the building's location in a cold climate and the intended use of the building. Energy consumption results are compared to those calculated in the Passive House Planning Package (PHPP) model completed for the building. Initial findings after an eighteen-month data collection period found that the exterior walls did not experience 100% relative humidity during the data collection period but that high readings of relative humidity (>80%) did occur. The measured annual heating and energy demand of the WIRL exceeded the predicted consumption values calculated in the PHPP model due to occupant behavior, mechanical system operation inefficiencies and discrepancies that exist between modeled vs actual climate conditions.

Keywords:
Passive House, Hygrothermal Behavior, Energy Efficiency, Cold Climate, Predicted vs Actual Energy Consumption

1. Introduction

The International Passive House standard for the construction of new buildings sets upper limits on the total heating demand and energy use a building may consume on an annual basis based on the conditioned floor area of the proposed design. To meet these requirements in cold climates, thick envelope assemblies that utilize enough thermal insulation are required in part with low air leakage levels. In addition, consideration must be given to the mechanical equipment and systems that will be installed in the building. To ensure the building achieves the established energy use targets, a computer model of the proposed building must be completed prior to the start of construction using the Passive House Planning Package (PHPP) software. Inputs to the model include envelope design, mechanical energy use, building location and airtightness value. Key outputs included the predicted annual heating demand (kWh/m^{2}a), total primary energy demand (kWh/m^{2}a), and air tightness of the building envelope (ACH@50pa). Previous research has shown that an extensive gap often exists between predicted and actual energy consumption in non-domestic buildings (Menezes, Cripps, Bouchlaghem & Buswell, 2012), (Bordass, Cohen & Field, 2004) & (Rees, 2017). In addition, there is a potential for long-term durability issues to develop in thick-wall assembly systems in heating dominated climates due to convective moisture transport through the building envelope assembly, leading to the growth of decay organisms (Pihelo, Kikkas & Kalamees, 2016), (Trainor, Smeagal, Straube & Parekh, 2016), (Watt, Sjoberg & Wahlgren, 2015) & (Ge & Straube, 2019). The purpose of this study is to investigate the hygrothermal performance and energy demand of the WIRL building following an eighteen month in-situ data collection period. The WIRL was completed in July of 2018 by the University of Northern British Columbia (UNBC) in Prince George, British Columbia, Canada. Prince George is located in Climate Zone 6B (ASHRAE 90.1-2010) with 4720 HDD under Cold-Dry conditions (Government of British Columbia Building and Safety Standards Branch, 2014). Built using a highly insulated envelope and airtight construction detailing, the building was constructed to provide students and faculty of the Integrated Wood Design Program with a facility that can accommodate research in the field of mass timber engineering and sustainability, including structural, seismic, acoustic and hygrothermal properties testing. The WIRL was built predominantly using wood and engineered wood-based products including glulam posts and beams and a locally sourced ceiling and wall truss system (Figure 1). The building consists of one large two-bay lab space with offices, classrooms and washroom facilities distributed between the first floor and a second-floor mezzanine (Figure 2). The building measures 10m in height and sits on top of a 31m x 31m concrete raft slab. The building is equipped with an elevator for access to the second-floor mezzanine to provide full accessibility. Machinery and equipment included in the predicted annual energy use of the WIRL include an overhead crane, three Universal Testing Machines (UTM) and a Hundegger brand Computer Numerical Controlled (CNC) cutting machine. In addition, the lab includes a 34 m^2 wood conditioning room that is equipped with ventilation and humidification in order to create an ideal environment for normalizing wood specimens to a consistent moisture content. Large shipments and deliveries can be received through an overhead bay door.

Figure 1. Wood Innovation Research Lab glulam post and beam structural system with vertical truss wall panel to be insulated on site.

The use of wood products for the structural and thermal assembly of a building has been shown to result in lower embodied energy, embodied carbon and greenhouse gas mitigation for buildings compared to the use of concrete or steel (Glover, White & Langrish, 2002), (Zeitz, Griffin & Dusicka, 2019) & (Börjesson & Gustavsson, 2000). A 2018 study of the global warming potential (GWP) of the WIRL building compared the total C02e of the building constructed using mass timber versus steel. The study found that the use of wood resulted in a 25% reduction in GWP when comparing the embodied energy of the two materials, and a 9% reduction in GWP when comparing the total lifecycle of the building, including operational energy (Wall & Wimmers, 2018). The WIRL will continue to have a low impact on the environment though energy-use savings due to its construction as a high-performance building certified under the Passive House certification system.

To help meet the low thermal energy demand requirements of the Passive House certification system, a unique vertical truss assembly was constructed for the exterior walls of the building. The finished walls measure 533mm deep and have a calculated U-value of 0.079 W/m^2K (RSI 12.66). The roof assembly used a similar design, with a flat truss assembly measuring 659mm thick and a U-value of 0.057 W/m^2K (RSI 17.54). The PHPP model completed for the WIRL calculated an annual heating demand of 12 $kWh/(m^2a)$ and an annual primary energy demand of 116 $kWh/(m^2a)$. Under specific circumstances when energy intensive equipment is used extensively in the summer months, a potential cooling load of 1 W/m^2 was also calculated.

Based on the final building design model and test results, the WIRL was deemed to have met all Passive House requirements and certification was achieved. The final airtightness value was recorded at 0.07 ACH@50Pa, a Canadian record for buildings certified under the Passive House program.

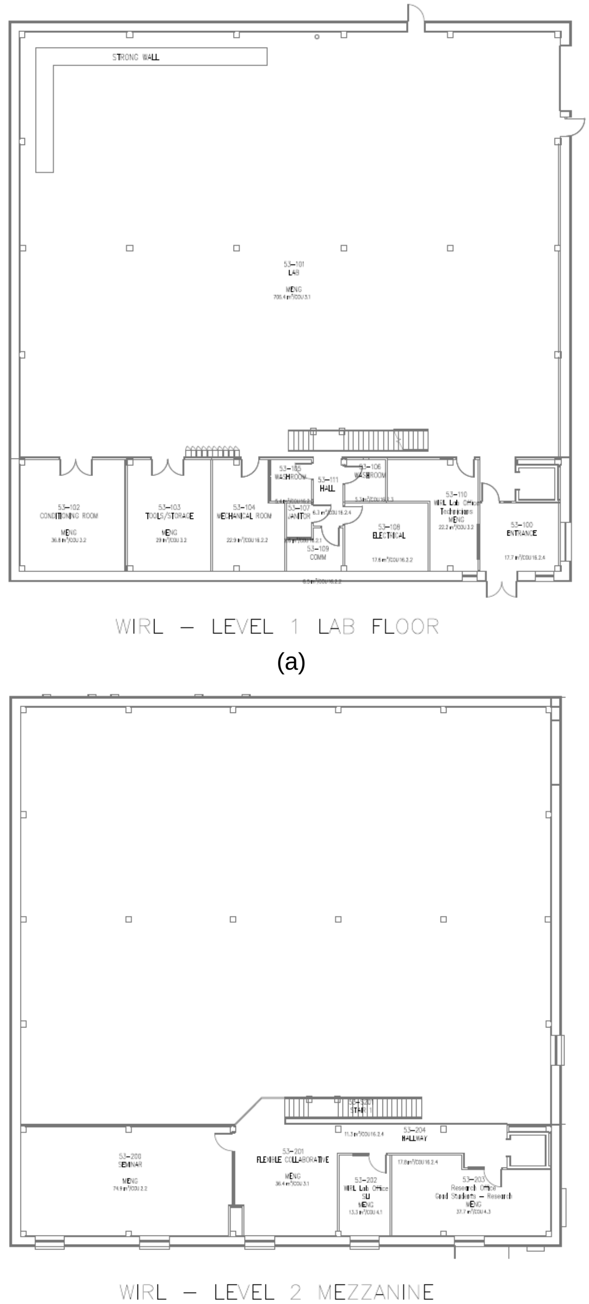

Figure 2. WIRL Level 1 (a) and Level 2 (b) floor plans

2. Methods

2.1 building energy use

The Passive House Planning Package (PHPP), a static simulation software, was used to estimate the annual energy and heating demand of the WIRL. Based on the construction of the building envelope, PHPP provides a precise simulation of the thermal energy demand of the building and detailed estimation of the energy load for all energy processes, including lighting, appliances, electronic equipment and mechanical systems operation. The completion of a PHPP model and confirmation of the estimated thermal energy demand and primary energy demand is mandatory for Passive House certification. Of interest for the PHPP model and certification of the WIRL was the energy consumption of the workshop and testing equipment. The use of saws, sanders, shapers and various other tools had to be estimated in addition to the standard operating mechanical equipment. The largest energy consumers were estimated to be the Hundegger CNC machine, the hydraulic power unit and actuators for the structural testing and the dust extraction system. The user cycles were calculated based on the estimated monthly use of each system averaged out over a one-year period following consultation with UNBC faculty.

To maintain a consistent indoor environment, the WIRL was separated into two climate-controlled zones. The first is the lab and research space, which was modeled at a temperature set point of 15.4°C. The second is the office and classroom space, which were modeled at 20°C. A lower set point for the lab space was deemed acceptable due to the nature and physical activities assumed for the occupants. Space heating and hot water are provided through a condensing natural gas boiler, while all electricity is provided through hydro power. Ventilation is provided to the building through two heat recovery ventilators (HRVs).

To measure the energy consumption of the WIRL, energy metering devices were installed on both the natural gas and hydro-electricity meters for the building. Individual meters for mechanical systems, laboratory equipment, lighting and miscellaneous loads were also installed. Energy consumption is reported on a monthly basis.

2.2 airtightness

Airtightness is an important part of building energy efficiency and the International Passive House certification. Air leakage through discontinuities in the primary air barrier can account for 30% or more of a building's heating and cooling costs (U.S. Department of Energy, 2019) and can lead to occupant discomfort and long term durability issues when moisture is transported into wall and ceiling assemblies through the process of air leakage (Janssens & Hens, 2003), (Desmarais, Derome & Fazio, 2000) & (Côté, 2016). To reduce heat loss from the building and encourage long-term durability, the Passive House certification program requires an airtightness value of 0.6 n50 1/h or less. The airtightness of the building is measured through the blower door test using the EN13829 and Passive House testing protocol.

2.3 exterior wall performance

The exterior walls of the WIRL were constructed using 533mm vertical truss panels. The uninsulated panels were constructed off-site and included the vertical truss assembly, interior sheathing and a vapour diffusion resistant adaptable membrane. Once on site, they were attached to the structural system and an exterior sheathing layer was applied with a proprietary weather-resistant barrier (WRB) sealed to the exterior face to control air leakage. Blown-in mineral fiber insulation was added from the exterior once the panels had been erected and the exterior sheathing and airtight membrane layers installed (Figure 3).

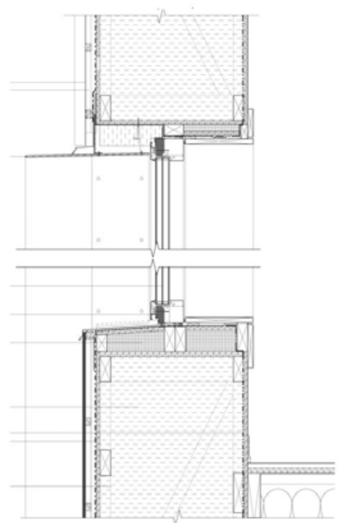

Figure 3. Cross-section diagram of WIRL wall

Six groups of three sensors were distributed vertically in both the north and south wall assemblies (Figure 4).

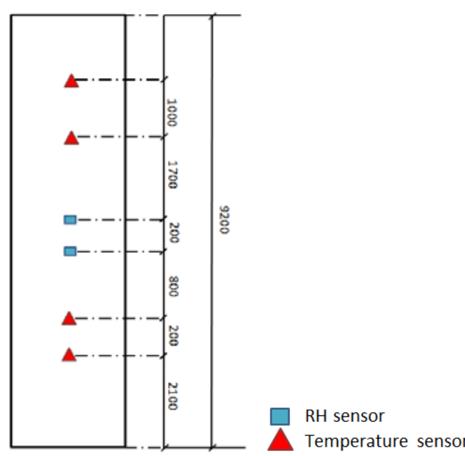

Figure 4. Elevation view of the vertical distribution of sensor bundles in north and south wall assembly panels.

Four of the six sensor arrangements in each wall were horizontally configured with two temperature and one humidity sensor (N01, N02, N05 and N06, and S01, S02, S05 and S06) (Figure 5b), and two arrangements were horizontally configured with two humidity and one temperature sensors (N03 and N04 and S03 and S04) (Figure 5a). For configurations N01, N02, N05 and N06 and S01, S02, S05 and S06, the temperature sensors are located on the exterior face of the interior OSB sheathing layer and the interior face of the exterior OSB sheathing layer, with the humidity sensor located in the center of the insulated assembly. The two additional sensor arrangements, N03 and N04 and S03 and S04, were configured with two humidity sensors and one temperature sensor. Here, the two humidity sensors are located on the exterior face of the interior OSB sheathing layer and the interior face of the exterior OSB sheathing layer, with the temperature sensor located in the center of the insulated assembly.

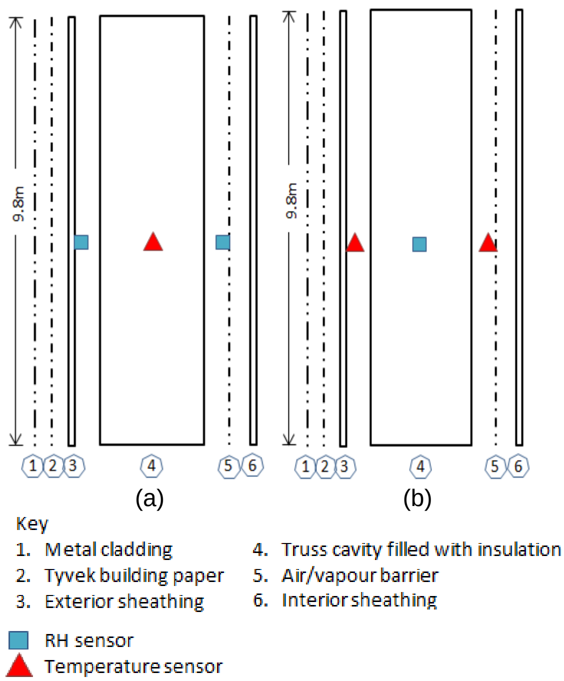

Figure 5. Cross-section view of the sensor placement in the north and south wall assemblies of the WIRL. Sensor groups N03 and N04 and S03 and S04 are configured as shown in (a). Sensor groups N01, N02, N05 and N06 and S01, S02, S05 and S06 are configured as shown in (b).

The sensor arrangements were integrated into the envelope of the building and were effectively non-removable after installation. The wiring for all sensors was bundled and brought through the wall assembly and connected to a Raspberry Pi controller, with care given to ensure a tight sealed was created where the wiring bundle penetrated the assembly. The length of wire used to connect each sensor to the controller was increased so that it ran parallel to the isotherms and the influence of the thermal conductivity of the wire on the sensor was reduced. By installing multiple sensors of the same configuration in both the north and south wall assemblies, it was ensured that a certain amount of redundancy existed both for data verification and continued data collection. In addition, vertical humidity and temperature profiles for each wall could be analyzed.

All sensors were chosen in order to communicate with the Inter- Integrated Circuit (I 2C) bus on a Raspberry Pi 3 controller, which allows multiple slave devices to communicate with a master device via the same data pin. MCP9808 temperature (accuracy of +/- 0.25 °C, range -40 °C to +125 °C).and Sensiron SHT31-D relative humidity and temperature sensors (RH accuracy of +/- 2%, temperature accuracy of +/- 0.3 °C) were used for this study.

3. Results

Results provided reflect data available during the first twenty months of data collection (July 2018 – March 2020). The gas consumption meter was installed and data collection began on December 6, 2018. The electrical consumption meters were installed and data collection began on July 13, 2018. Building energy and heating fuel consumption values are reported for a one-year period (January 31, 2019 – January 31, 2020).

Following a review of the heating fuel and energy use consumption values recorded during the data collection period, it was discovered that a significant gap existed between April – December 2019 due to power failures and communication errors. Because the recorded values for the building are cumulative, annual energy and heating consumption could be calculated using the values available once data collection resumed. Comparative monthly data values are presented for those months where data is available.

The projected annual heating demand for the WIRL in PHPP was 12 kWh/(m^2a). Based on the data collected from the natural gas meter, the WIRL building had an annual heating demand of 26.6 kWh/(m^2a). The difference in monthly heating demand values for four months is shown in Figure 6.

The projected final annual energy demand for the WIRL in PHPP was 40.8 kWh/(m^2a), excluding heating energy demand. In comparison, the total energy consumption for the building between January 31, 2019 and January 31, 2020 was 76.99 kWh/(m^2a), excluding heating energy consumption. Because the actual energy consumption of the WIRL cannot be broken down sufficiently to apply the appropriate PE factors used in PHPP, only the final energy demand will be compared in this study. The possible sources of the discrepancy between predicted versus actual heating and energy demand are discussed in the next section.

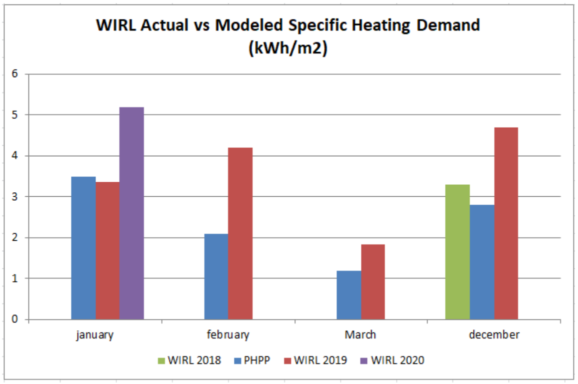

Figure 6. WIRL specific heating demand calculated vs actual energy consumption

Following completion of the building in July of 2018, the WIRL achieved a final airtightness rate of 0.07 n50 1/h. Points of air leakage through the envelope were identified and included minor penetrations through the wall assembly. Much of the leakage detected was around the perimeter of the overhead bay door installed on the east wall of the building. To measure what, if any changes had occurred to the airtight layer since construction was completed, a second, follow up airtightness test was performed on Feb. 6, 2019. The results are shown in Table 1. As per testing protocol established under the Passive House certification system, both a pressurization and depressurization test were completed to reflect all possible areas of leakage within the envelope.

Test Direction	**Air changes at 50 Pa, n_{50} 1/h**
Pressurization	0.1128
Depressurization	0.1717
Final	0.1423

Table 1. Results of the follow-up airtightness testing performed on the WIRL building on February 6, 2019

Following a review of the data collected by the six sensor arrangements installed in both the north and south walls of the WIRL, it was discovered that sensor configuration S01 had not transmitting data and no values had been recorded. Sensor configuration S05 transmitted data for two days, July 19 and July 20, 2018, before encountering a malfunction or error that resulted in no further data being reported. Sensor configuration N02 did not transmit any data after January 23, 2020. Additionally, the RH sensor located towards the exterior side of the assembly in configuration S03 did not transmit data after January 12, 2019.

The data collected from the six sensor arrangements showed that at no point during the data collection period of July 18, 2018 to March 4, 2020 was 100 percent relative humidity achieved in either the north or south wall assembly. The maximum relative humidity values were recorded by sensor N05 on January 19, 2020 at 09:34, with a value of 84.84%, and sensor S03 on January 7, 2019 at 17:00 at 94.24%. The dates of these readings correspond to one of the coldest weather periods recorded during the data collection period.

4. Discussion

4.1 building energy use

Currently, 63% of residential and 55% of commercial/institutional energy end use comes from space heating demands (Natural Resources Canada, 2016). By improving the thermal performance of a building's envelope and increasing the airtightness rate, a significant impact can be made on a building's greenhouse gas emissions over its operational lifespan (Itard, 2009) & (T. Sharmin, Li, Ganev, & Nikolaidis, 2014).

When evaluating the predicted specific heating demand value calculated by PHPP versus the recorded heating energy consumption, we can see that a performance gap exists (Figure 6). Performance gaps in modeled versus in-situ data have previously been discussed regarding building energy use (Menezes, Cripps, Bouchlaghem, & Buswell, 2012) & (Rees, 2017). Here, we broaden the use of the term to include thermal heating demand. It is important to review the assumptions made by PHPP in calculating the specific heating demand for the building so that we may better understand the possible source(s) of this performance gap. Validation of building energy use models with in-situ collected data can help improve the accuracy of future building models including user inputs and energy use predictions.

To calculate the heating demand of a building, the ISO 13790 standard is used by PHPP to balance all thermal losses through opaque and transparent envelope components, ventilation losses and solar heat gains as well as internal heat gains to establish the remaining specific heating (or cooling) demand and the heating (or cooling) load of the mechanical equipment. For the calculation of the internal heat gains the type, power and user intervals of all equipment such as lights, plug loads for computers and miscellaneous equipment are calculated.

The primary concern in deriving the energy consumption values of the lab testing equipment was to ensure that their use would not lead the predicted annual energy demand of the building to exceed certification requirements. Therefore, estimates of the annual energy use were based on the frequent use of the equipment in order to provide a conservative energy consumption estimate while still ensuring the certification requirements would be met. Based on the estimated annual use of this equipment, the total internal heat gains calculated by PHPP were 17.7 kWh/(m^2a).

The estimated annual energy demand of all equipment in the WIRL was 39 246 kWh/a. For the period of January 31, 2019 – January 31 2020, the actual recorded energy consumption of this equipment was 49 965 kWh. The annual energy demand of the lighting system was also underestimated, with an estimated energy demand of 6 043 kWh/a, while the recorded energy consumption for January 31, 2019 – January 31 2020 was 9 821 kWh.

As a result of the increase in energy use of the equipment and lighting, an increase in internal heat gain will occur, decreasing the demand on the building's heating system. PHPP accounts for the heat gains from the equipment and lighting located inside the thermal envelope and reduces the demand on the heating system accordingly. When the values in the PHPP model were adjusted to reflect the actual annual energy consumption of both the lighting and lab equipment, the total available internal heat gain for the building was increased from 17.7 kWh/(m^{2}a) to 21.8 kWh/(m^{2}a). As a result, the estimated annual heating demand of the building decreased from 11.4 to 8.5 kWh/(m^{2}a) (Figure 7).

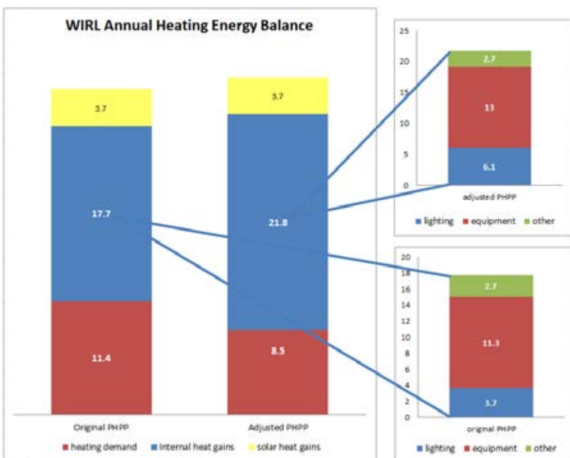

Figure 7. Available internal heat gains and estimated total building heating demand kWh/(m^{2}a).

PHPP's estimate of the annual heating demand of the WIRL does not reflect the actual heating energy consumption as recorded between January 31, 2019 and January 31, 2020, which was 26.6 kWh/(m^{2}a). As a result of this significant discrepancy between predicted and actual heating energy consumption, further investigation was taken to identify the cause(s) for the additional heating energy consumption. After consulting with staff and reviewing the annual operations of the building, several discrepancies were found between the PHPP model and the in-situ performance of the WIRL. These include:

1. The operating temperature of the lab space. When a review of the building operations was conducted, it was found that the lab was being operated at a temperature set point of 18°C. The PHPP model was completed using an operating temperature of 15.4°C.
2. The climate data used in the PHPP model compared to that which was experienced during the reporting period (January 31, 2019 – January 31, 2020). On average, the climate data used in PHPP model shows a good fit with the ambient monthly temperatures (Figure 8). However, February 2019 shows a particularly large divergence between the two values, which can be accounted for in the fact that it was the coldest February on record in the city's history, with an average temperature of -17.7°C, while the ambient monthly temperature used by PHPP is -3.9°C.

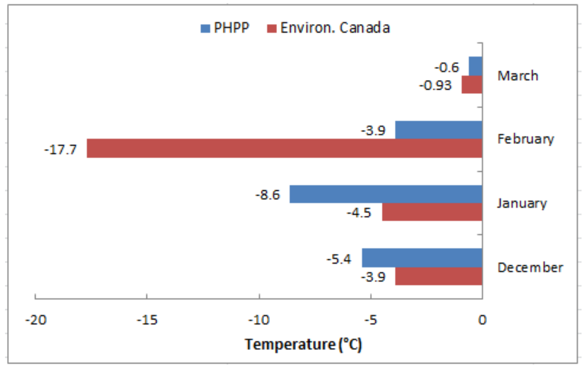

Figure 8. Modeled ambient temperature vs. actual weather data for WIRL building.

3. Discussion with the faculty who use the WIRL daily revealed two additional sources for the discrepancy in the heating energy demand. The first is the use of the faculty office and student classroom space, which is commonly occupied. These spaces have a temperature set point of 20°C; however, the doors connecting these spaces to the adjacent lab space are commonly left open. Due to the operating temperature difference between these spaces, heat loss from the offices and classrooms is likely to occur, increasing the heating energy consumption. In addition, deliveries to the lab space via the overhead bay door were not accounted for in the PHPP model. Deliveries of mass timber supplies and testing equipment require the door to be open for extensive periods of time, causing significant heat loss from the lab during the heating months when these deliveries occur.
4. The use of the dust extraction system, which is operated during the cutting and machining of wood, requires the exhausted air to be circulated through two filtration systems, one of which is located exterior to the building, before it is returned to the building. Additional heat loss from the building that occurs during the use of the dust extraction recirculation process was not accounted for in PHPP.
5. Discussion with the University building management team found that the mechanical systems for the WIRL were not operating in an optimal manner based on user behavior and control system programming. The generation of additional heat from equipment use and plug loads in the building is rejected from the building through the use of a fluid cooler system, resulting in less of the internal heat gain energy being used

to offset the heating demand load as calculated by PHPP.

The operating temperature of the lab space was increased to 18°C in the PHPP model; no adjustments were made to the climate data or to account for user behavior or mechanical system operation in the building. As a result, the predicted annual heating energy demand of the WIRL increased to 13.2 kWh/(m^{2}a). When the impact of the increased air leakage of the envelope was also accounted for and the airtightness value in the PHPP model increased to 0.14 ACH @50Pa, the predicted annual heating energy demand increased to 13.8 kWh/(m^{2}a). Because a significant portion of the internal heat gains calculated by PHPP is not available to the building, we believe the remaining discrepancy between the actual heating energy consumption and the predicted energy demand may be accounted for in mechanical system operation in addition to occupant behavior, irregular use of the lab space and variations in ambient monthly temperatures for the reported period compared to those used in the PHPP model.

Following the adjustment of the PHPP model to reflect the actual energy use for the building, the adjusted final predicted energy demand of the PHPP model was 80.3 kWh/(m^{2}a). This result shows strong correlation with the annual energy consumption of the building, which was 76.99 kWh/(m^{2}a) for the period of January 31, 2019 to January 31, 2020.

4.2 airtightness

The permeability of the airtight layer in the WIRL building envelope increased from 0.07 n50 1/h to 0.14 n50 1/h as determined by the follow-up airtightness test conducted 7 months after the completion of the building. To determine the location(s) of the additional air leakage, a thermographic assessment of the building envelope was conducted in conjunction with the follow-up airtightness test. At the time of testing the exterior temperature measured -29.0°C and the interior temperature was +17.5°C.

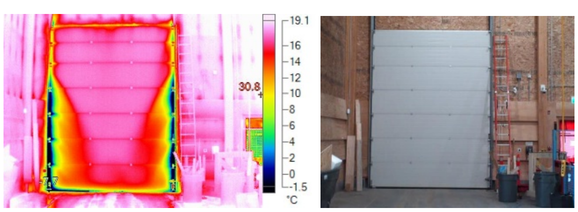

(a) (b)

Figure 9. Thermographic image of the WIRL bay door (a) and corresponding visible light image (b) taken during the follow up air leakage test conducted on Feb. 6, 2019.

Figure 9 shows the large bay door for semi-trucks. Through airtightness testing we established already that this door, even though the highest quality available today, is still a weak point in terms of thermal performance and air tightness. The picture shows the infiltration of cold air in the lower section of the door symmetrically on both sides. It can be assumed that during regular operating conditions of the building this area is a significant source of heat loss.

Figure 10 shows cold air infiltrating mainly on the opening side of the north wall entry door due to a malfunctioning seal between the door and frame. These results highlight the importance of long-term performance reviews to maintain consistent airtightness results following building occupancy and use.

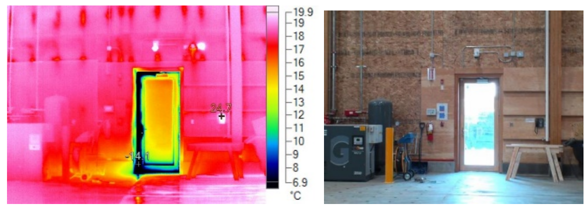

(a) (b)

Figure 10. Thermographic image of the north entry door (left) and corresponding visible light image (right) taken during the follow up air leakage test conducted on Feb. 6, 2019.

4.3 exterior wall performance

The values recorded by the RH sensor located towards the exterior side of the assembly in sensor configuration S03 were not found to be consistent with the other values recorded by the sensors in the south wall (Figure 11). For the date on which the highest RH value was recorded by the sensor, we expect a similar value from the sensor located in the same position in sensor configuration S04. On January 7, 2019, when the sensor in configuration S03 recorded an RH value of 94.24%, the sensor in the same position in configuration S04 recorded a RH value of 65.98%. An additional check of the RH sensors found in the center of the wall assembly in sensor configurations S02 and S06 for the same date and time show values of 68.52% and 51.13% RH, respectively.

The source of the discrepancy in the values recorded by the exterior RH sensor in configuration S03 is unknown. One possible explanation is a discontinuity in the air barrier system on the exterior side of the assembly close to the sensor location, allowing either air or moisture to penetrate the assembly, causing a localized increase in relative humidity values. Due to the known airtightness of the building, however, this is not believed to be the cause. Another possible cause for the high relative humidity values is insulation installation defects. Should an air gap exist around the location where the sensor is installed, a localized increase in recorded RH values may occur due to a decrease in air temperature (Bankvall, 1978) & (W. C. Brown, 1993). A third and final possibility is incorrect calibration of the sensor before installation or sensor malfunction following installation. Because the sensor is not accessible, recalibration is not possible. Given that the results from this sensor in configuration S03 are not consistent with those reported by configurations

S04, S02 and S06, we believe the values reported may be discarded.

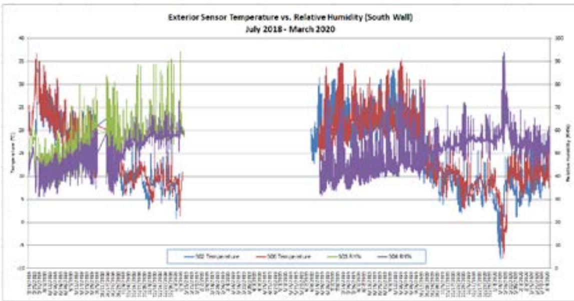

Figure 11. South wall exterior sensors (S02, S06, S03 and S04) relative humidity vs temperature.

The values recorded by the sensors located towards the exterior side of the assembly in the six north wall sensor configurations are shown in Figure 12.

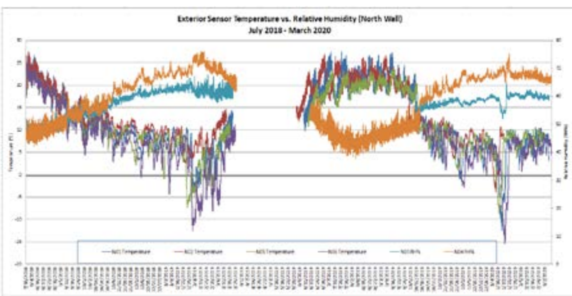

Figure 12. North wall exterior sensors (N01, N02, N03, N04, N05 and N06) relative humidity vs temperature.

The values recorded by the sensors in both the south and north walls show that the temperature and relative humidity of the exterior side of the wall assembly are largely governed by the exterior air temperature, with large fluctuations recorded by the sensors in the south wall configurations due to solar gain on the building façade. The values recorded by the sensors located towards the interior side of the north and south walls, not shown here, show similar results, with the recorded values reflective of the interior climate conditions of the lab.

The relative humidity values recorded by all sensors in configurations N01-N06 for the period of July 18, 2018 – March 4, 2020 are shown in Figure 13. From the values recorded by the sensors in configurations N01, N02, N05 and N06 we can see that the relative humidity of the center of the wall closely follows the behavior of the exterior side of the assembly and is largely governed by the exterior air temperature. In addition, a stratification of the results can be seen, with higher relative humidity values recorded by the sensors at a lower position vertically in the wall. These results are also reflected in the temperature values recorded by the sensors in the north wall, shown in Figure 14, with lower temperature values recorded by the sensors at a lower position in the assembly. This stratification of temperature and relative humidity may be due to a similar stratification of air temperature in the lab space adjacent to the assembly and subsequent conductive and radiant heat transfer, convective air movement within the wall assembly itself, or uneven moisture distribution within the assembly materials. As the initial moisture content of the envelope assembly materials was not taken and interior temperature sensors were not installed on the wall assemblies, conclusive evidence cannot be given as to the cause for these results.

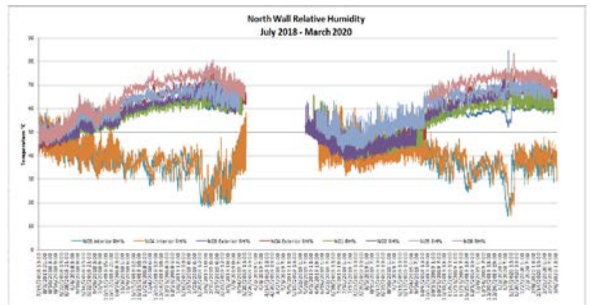

Figure 13. Recorded relative humidity in the north wall of the WIRL (July 2018 – March 4, 2020)

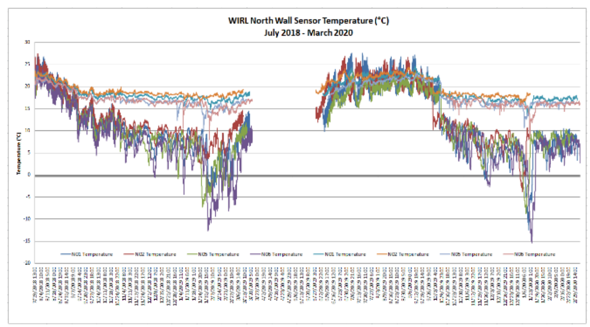

Figure 14. Recorded temperatures in the north wall of the WIRL (July 2018 – March 4, 2020)

Critical moisture levels for mould growth in building materials have been reported as low as 75-80% RH, however sustained periods of high relative humidity are required for significant growth (>12weeks) (Johansson, Ekstrand-Tobin, Svensson, & Bok, 2012). Although the peak relative humidity value recorded by N06 is high enough to support mould growth in the exterior sheathing of the wall assemblies, the critical moisture level was not sustained for a period deemed sufficient to allow growth to occur. Annex 14 of the International Energy Agency (IEA) recommends that the surface relative humidity of an assembly be kept below 80% on a monthly mean basis (Hens, 1992). Similarly, ASHRAE Standard 160 recommends a 30-day running average surface relative humidity be less than 80% when the average surface temperature for the same period is between 5 and 40°C (ASHRAE, 2009). For the data collection period, the highest monthly mean relative humidity level occurred in sensor configurations N06 and S03, with values of 74.30% and 71.58%, respectively. Therefore, for the reported data collection period we feel confident that the exterior wall assembly has performed sufficiently and not experienced conditions susceptible to decay organism growth.

5. Conclusion

The annual heating and primary energy demand of UNBC's Wood Innovation and Design Center exceed the values predicted by the PHPP model. The discrepancies are primarily due to assumed energy consumption values of lighting and laboratory shop equipment as well as mechanical systems operations, occupant behavior and differences in experienced climatic values for the reported year. The sensors that were installed in the north and south walls demonstrate good hygrothermal behavior, with no record of 100% relative humidity occurring in the assembly and monthly average values below 80% relative humidity. Ongoing data analysis will allow for a better understanding of the long-term hygrothermal performance of the thick-wall assembly under variable climate and interior operating conditions. The loss of monthly data records during 2019 resulted in a poor comparison of the building performance on a monthly basis. Variations in annual climate conditions can result in discrepancies between modeled versus actual performance; therefore, a longer data collection period should result in a more accurate comparison between the building's performance and PHPP modeled values.

It is important that the intended use of a building is taken into consideration when designing and constructing high performance timber-frame wall assemblies. The function of the WIRL as a research and testing facility allows for consistent interior operating climate conditions, including temperature and humidity. The exterior wall assembly has been shown to function well and not present risk for extended periods of high relative humidity. The results show that the long-term durability of high-performance buildings constructed to meet low energy-use standards like the Passive House certification require appropriate planning and design. Should the given wall assembly be used in the construction of a structure that experiences other climate or operating parameters, it may perform differently. Proper hygrothermal modeling of high-performance building assemblies should always be conducted to ensure they will perform appropriately for the climate and construction scenario they will operate under.

The results show a significant performance gap exists between the energy use and heating energy consumption of the WIRL compared to the values used in the PHPP model completed prior to the construction of the building. The reported building energy consumption used in this analysis contains values collected over a one-year time period. The function of the WIRL as an institutional research facility results in variable energy consumption of the building on an annual basis. The results of this study highlight the challenges that exist in the use of the International Passive House system for the certification of an institutional research facility. The variability in annual energy consumption of laboratory equipment and occupant behavior can result in significant discrepancies between the predicted and actual energy consumption of the building. When equipment is used frequently, internal heat gains play a significant role in reducing the heating energy demand of the building, however occupant behavior, annual climate variations and irregular building use patterns may result in heating energy consumption discrepancies. The recommissioning of building mechanical equipment after one year of operation and occupancy may allow for additional energy savings and performance optimization. Long-term monitoring of energy use data is required to see if the Passive House certification program is an adequate tool for estimated building energy use and certification for buildings of these types. The building envelope performance and unique design for this application worked well, however.

Acknowledgements

This research was funded by Forestry Innovation Investment Ltd. The authors thank UNBC's Facilities Management team and UNBC staff for providing information and support throughout the data collection and analysis that was used in the writing of this case study.

References

ASHRAE. (2009). *Criteria for Moisture-Control Design Analysis in Buildings.* Atlanta: American Socieity of Heating, Refrigeration and Air-Conditioning Engineers.

Bankvall, C. G. (1978). Forced Convection: Practical Thermal Conductivity in an Insulated Structure Under the Influence of Workmanship and Wind. In A. S. Material, *Thermal Transmission Measurements of Insulations* (pp. 409-425). West Conshohocken: ASTM International.

Bordass, B., Cohen, R., & Field, J. (2004). Energy performance of non-domestic buildings - closing the credibility gap. *International conference on improving energy efficiency in commercial buildings.* Frankfurt.

Börjesson, P., & Gustavsson, L. (2000). Greenhouse gas balances in building construction: wood versus concrete from life-cycle and forest land-use perspectives. *Energy Policy*, 575-588.

Côté, J.-F. (2016). Highly permeable air barriers may increase the risk of condensation in wall assemblies. *RCI, Inc. 31st International Convention & Trade Show.* Orlando: International Institute of Building Enclosure Consultants.

Desmarais, G., Derome, D., & Fazio, P. (2000). Mapping of Air Leakage in Exterior Wall Assemblies. *Journal of Building Physics*, 132-154.

Ge, H., & J. Straube, L. W. (2019). Field study of hygrothermal performance of highly insulated wood-frame walls under simulated air leakage. *Building and Environment*, 106202.

Glover, J., White, D. O., & Langrish, T. A. (2002). Wood versus Concrete and Steel in House Construction: A Life Cycle Assessment. *Journal of Forestry*, 34-41.

Government of British Columbia Building and Safety Standards Branch. (2014, July 23). *Determining ASHRAE 90.1-2010 Climate Zones.* Retrieved from Government of British Columbia: https://www2.gov.bc.ca/assets/gov/farming-natural-resources-and-industry/construction-industry/building-codes-and-standards/bulletins/b14-01_determining_ashrae_901-2010_climate_zones.pdf

Hens, H. (1992). IEA Annex 14: Condensation and Energy. *Journal of Thermal Insulation*, 261-273.

Itard, L. C. (2009). Embodied and operational energy use of buildings. *Lifecycle Design of Buildings, Systems and Materials* (pp. 77-84). Enschede: International Council for Building Research Studies and Documentation.

Janssens, A., & Hens, H. (2003). Interstitial condensation due to air leakage: A sensitivity Analysis. *Journal of Building Physics*, 15-29.

Johansson, P., Ekstrand-Tobin, A., Svensson, T., & Bok, G. (2012). Laboratory study to determin the critical moisture level for mould growth on building materials. *International Biodeterioration & Biodegradation*, 23-32.

Menezes, A. C., Cripps, A., Bouchlaghem, D., & Buswell, R. (2012). Predicted vs. actual energy performance of non-domestic buildings: using post-occupancy evaluation data to reduce the performance gap. *Applied Energy*, 355-364.

Natural Resources Canada. (2016). *Energy Efficiency Trends in Canada 1990 to 2013.* Ottawa: Government of Canada.

Pihelo, P., Kikkas, H., & Kalamees, T. (2016). Hygrothermal performance of highly insulated timber-frame external walls. *Energy Procedia*, 685-695.

Rees, S. J. (2017). Closing the performance gap through better building physics. *Building services engineering research and technology*, 125-132.

T. Sharmin, M. G., Li, X., Ganev, V., & Nikolaidis, I. (2014). Monitoring building energy consumption, thermal performance, and indoor air quality in a cold climate region. *Sustainable Cities and Society*, 57-68.

Trainor, T., Smeagal, J., Straube, J., & Parekh, A. (2016). Measured and predicted moisture performance of high-wall assemblies in cold-climates. *Thermal performance of the exterior envelopes of whole buildings XIII.* Clearwater: American Society of Heating, Refrigeration and Air-conditioning Engineers.

U.S. Department of Energy. (2019). *Air Sealing for New Home Construction.* Retrieved from Energy.gov: https://www.energy.gov/energysaver/air-sealing-your-home/air-sealing-new-home-construction

W. C. Brown, M. T. (1993). Measured Thermal Resistance of Frame Walls with Defects in the Installation of Mineral Fibre Insulation. *Thermal Insulation and Building Envelopes*, 318-339.

Wall, S., & Wimmers, G. (2018). *A comparative LCA of the Wood Innovation Research Lab: An Industrial PH for cold climates.* Retrieved from https://www.researchgate.net/publication/339886779_A_comparative_LCA_of_the_Wood_Innovation_Research_Lab_An_industrial_PH_for_cold_climates

Watt, D., Sjoberg, S., & Wahlgren, P. (2015). Hygrothermal performance of a light weight timber wall assembly with an exterior air barrier. *Energy Procedia*, 1419-1424.

Zeitz, A., Griffin, C. T., & Dusicka, P. (2019). Comparing the embodied carbon and energy of a mass timber structure system to typical steel and concrete alternatives for parking garages. *Energy & Buildings*, 126-133.